

Structural and Kinetic Studies of Sugar Binding to Galactose Mutarotase from *Lactococcus lactis**

Received for publication, August 16, 2002
Published, JBC Papers in Press, September 5, 2002, DOI 10.1074/jbc.M208395200

James B. Thoden^{‡§}, Jungwook Kim[¶], Frank M. Raushel[¶], and Hazel M. Holden[‡]

From the [‡]Department of Biochemistry, University of Wisconsin, Madison, Wisconsin 53706-1544 and the [¶]Department of Chemistry, Texas A&M University, College Station, Texas 77842-3012

Galactose mutarotase catalyzes the conversion of β -D-galactose to α -D-galactose in the Leloir pathway for galactose metabolism. The high resolution x-ray structure of the dimeric enzyme from *Lactococcus lactis* was recently solved and shown to be topologically similar to the 18-stranded, anti-parallel β -motif observed for domain 5 of β -galactosidase. In addition to determining the overall molecular fold of galactose mutarotase, this initial investigation also provided a detailed description of the electrostatic interactions between the enzyme and its physiologically relevant substrate, galactose. Specifically, the side chains of His-96 and His-170 were shown to be located within hydrogen bonding distance to the C-5 oxygen of the substrate, while the carboxylate of Glu-304 was positioned near the C-1 hydroxyl group of the sugar. On the basis of this initial study, a possible role for Glu-304 as the general acid/base group in catalysis was put forth. Here we describe the combined x-ray crystallographic and kinetic analyses of *L. lactis* galactose mutarotase complexed with D-glucose, D-fucose, D-quinovose, L-arabinose, or D-xylose. These investigations have revealed that there are several distinct binding modes for these sugars, which are dependent upon the spatial orientation of the C-4 hydroxyl group. In those sugars with the same C-4 hydroxyl group orientation as galactose, their C-1 hydroxyl groups are invariably located near Glu-304. For those sugars, which have the same C-4 hydroxyl group configuration as glucose, the C-1 hydroxyls are typically located near Asp-243. These different binding modes correlate with both the observed kinetic parameters and the presence or absence of a hydrogen bond between the guanidinium group of Arg-71 and the C-4 hydroxyl group of the sugar ligand.

Galactose mutarotase plays a key role in the Leloir pathway for galactose metabolism by catalyzing the conversion of β -D-galactose to α -D-galactose (1). The enzyme has been isolated from diverse sources such as *Penicillium notatum* (2, 3), *Escherichia coli* (4), hog kidney and lens (5, 6, 7), green pepper (8), and bovine kidney cortex (9). Additionally, genes encoding en-

zymes with mutarotase activities have now been identified in *Acinetobacter calcoaceticus* (10), *Streptococcus thermophilus* (11), *Lactobacillus helveticus* (12), *Haemophilus influenzae* (13), and *Lactococcus lactis* (14), among others. A possible catalytic mechanism for galactose mutarotase, first suggested by Hucho and Wallenfels (15) and outlined in Scheme 1, involves the abstraction of a proton from the C-1 hydroxyl group of the sugar by an enzymatic base and donation of a proton to the C-5 oxygen by a side chain acidic group thus resulting in ring cleavage. Subsequent rotation about the C-1/C-2 bond, followed by abstraction of the proton on the C-5 oxygen and donation of a proton back to the C-1 oxygen leads to product formation.

The crystal structure of the enzyme from *L. lactis* has recently been solved to high resolution, both in the unbound state and complexed with galactose (16). A ribbon representation of one subunit of this dimeric enzyme is displayed in Fig. 1a. The overall fold of the monomer is dominated by extensive layers of β -sheet and, despite no amino acid sequence homology, is topologically similar to the 18-stranded, anti-parallel β -motif observed for domain 5 of β -galactosidase (17). This three-dimensional architecture has also been observed in copper amine oxidase (18), hyaluronate lyase (19), chondroitinase (20), and maltose phosphorylase (21).

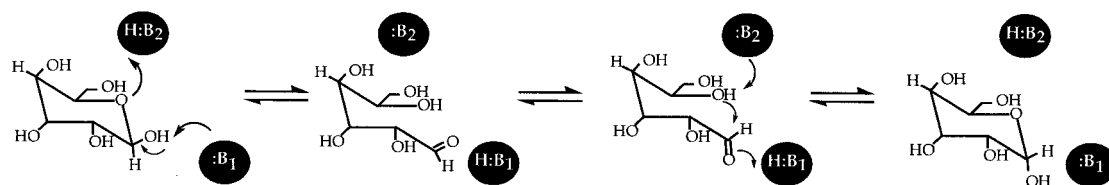
As demonstrated by this first x-ray crystallographic analysis of a galactose mutarotase, there are few structural changes that accompany sugar binding. Indeed, the sugar substrate is accommodated within the active site via movement of solvent molecules rather than major perturbations of side chain conformations except for that of Phe-279. The aromatic group of Phe-279 shifts somewhat to accommodate the C-1 hydroxyl group of galactose in its α -anomeric configuration. The electron density corresponding to the galactose ligand indicated the presence of both anomers in the active site. A close-up view of the mutarotase active site with bound α,β -D-galactose is presented in Fig. 1b. Both His-96 and His-170, which are strictly conserved among mutarotase amino acid sequences, are located within 3 Å of the C-5 oxygen of the sugar. Additionally, Glu-304 is situated at ~ 2.7 Å from the C-1 hydroxyl group of galactose. From this initial investigation, it was postulated that Glu-304 functions to initiate the reaction. Since both His-96 and His-170 lie within hydrogen bonding distance to the C-5 oxygen, either is positioned to serve as the active site acid required to protonate the C-5 oxygen, and it was not apparent from this first structure which one serves in such capacity.

In addition to catalyzing the physiologically relevant conversion of β -D-galactose to α -D-galactose, mammalian mutarotases have been shown to act upon D-glucose, D-xylose, and L-arabinose as well (5, 9, 22). The structures of these sugars are depicted in Scheme 2. Here we present both kinetic and x-ray crystallographic data on the binding of various sugars to galactose mutarotase from *L. lactis*. The first

* This work was supported in part by National Institutes of Health Grants DK47814 (to H. M. H.) and DK30343 (to F. M. R.). The costs of publication of this article were defrayed in part by the payment of page charges. This article must therefore be hereby marked "advertisement" in accordance with 18 U.S.C. Section 1734 solely to indicate this fact.

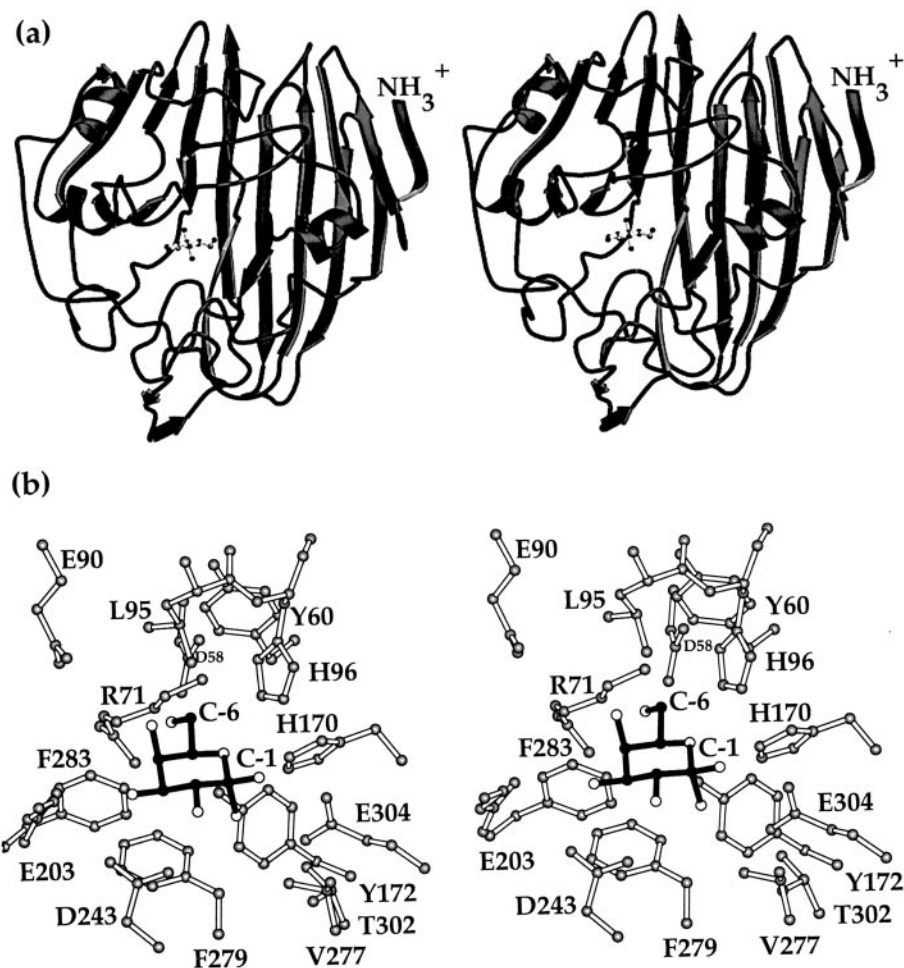
The atomic coordinates and structure factors (code 1MMU, 1MMX, 1MMY, 1MMZ, and 1MNO) have been deposited in the Protein Data Bank, Research Collaboratory for Structural Bioinformatics, Rutgers University, New Brunswick, NJ (<http://www.rcsb.org/>).

§ To whom correspondence should be addressed: Dept. of Biochemistry, University of Wisconsin, 443 Babcock Dr., Madison, WI 53706-1544. Tel.: 608-262-0529; Fax: 608-262-1319; E-mail: JBThoden@facstaff.wisc.edu.



SCHEME 1

FIG. 1. Structure of galactose mutarotase from *L. lactis*. Shown in *a* is a ribbon representation of one subunit of galactose mutarotase. The bound galactose molecule is depicted in a ball-and-stick representation. A close-up view of the active site within 5 Å of galactose is displayed in *b*. Ordered water molecules surrounding the sugar ligand were omitted for figure clarity. All figures were prepared with the software package MOLSCRIPT (26).



structure to be solved in this investigation was that of the mutarotase complexed with glucose. Surprisingly, the glucose ligand bound in a quite unexpected manner with its C-6 hydroxyl group located near His-96 and His-170 and its C-1 hydroxyl group lying within hydrogen bonding distance of Arg-71, Glu-203, and Asp-243. This alternate binding mode, as compared with that of galactose, inspired the additional series of structural and kinetic analyses presented here. Specifically, the structures of the enzyme complexed with D-fucose, D-quinovose, L-arabinose, or D-xylose have now been determined to 1.9-Å resolution or better, and the kinetic constants for sugar binding have been measured. As can be seen from Scheme 2, both D-fucose and D-quinovose represent C-6 deoxy sugar mimics of galactose and glucose, respectively. Likewise, L-arabinose and D-xylose serve as five-carbon analogs of galactose and glucose, respectively. Taken together, these investigations demonstrate that sugar binding within the active site cleft of galactose mutarotase is varied and that the different binding modes can, in part, be correlated with the observed kinetic parameters and with the spatial orientations of the C-4 hydroxyl groups.

EXPERIMENTAL PROCEDURES

Protein Purification and Crystallization—The necessary protein required for these studies was expressed in *E. coli* and purified as described previously (16). Large single crystals of the unliganded form of the enzyme were routinely grown by vapor diffusion against precipitant solutions containing 15–19% poly(ethylene glycol) 5000 methyl ether and 100 mM MES¹ (pH 6.0). Enzyme concentrations were typically 17.5 mg/ml. The crystals achieved maximum dimensions of 0.3 × 0.3 × 0.2 mm in ~1–2 weeks and belonged to the space group P2₁2₁2₁ with typical unit cell dimensions of *a* = 44.8 Å, *b* = 76.3 Å, and *c* = 211.1 Å. The asymmetric unit contained one dimer.

Structural Analyses of the Galactose Mutarotase-Sugar Complexes—Crystals of the unbound form of galactose mutarotase were harvested from hanging drop experiments and equilibrated in a synthetic mother liquor composed of 20% poly(ethylene glycol) 5000 methyl ether, 200 mM NaCl, 100 mM MES (pH 6.0), and a 100 mM concentration of the appropriate sugar. After equilibration for 24 h at 4 °C, x-ray data sets were collected to high resolution at 4 °C with a Bruker HISTAR area detector system equipped with Göbel focusing optics. The x-ray source was CuK α radiation from a Rigaku RU200 x-ray generator operated at

¹ The abbreviation used is: MES, 2-(*N*-morpholino)ethanesulfonic acid.

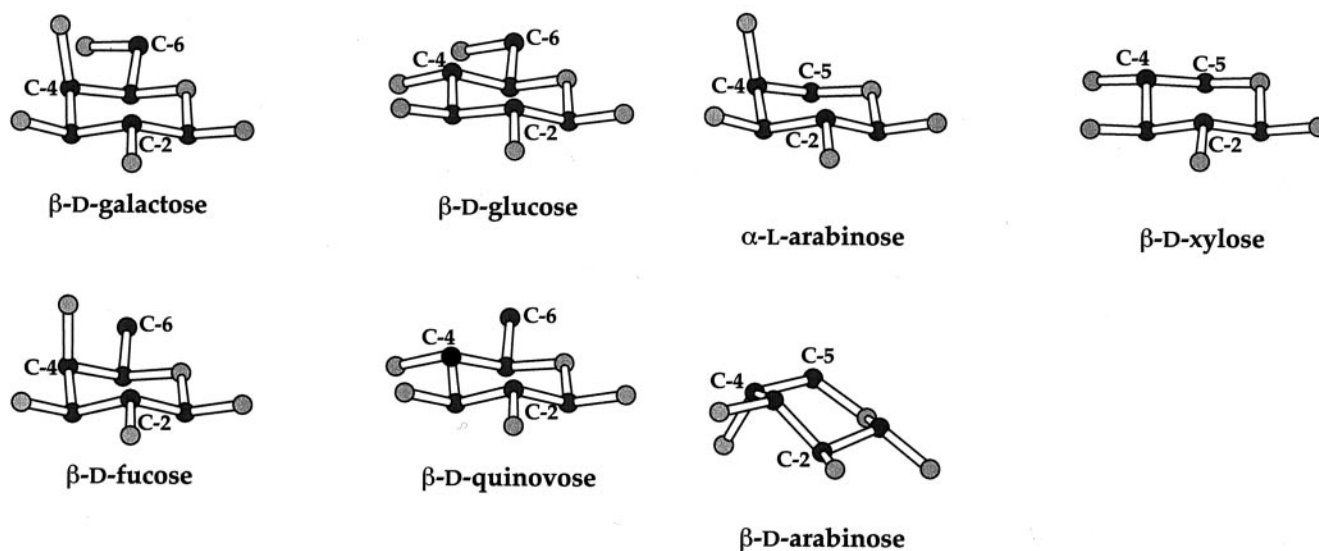


TABLE I
X-ray data collection statistics

X-ray data set	Resolution Å	Independent reflections	Completeness %	Redundancy	Avg $I/\text{Avg } \sigma(I)$	R_{sym}^a
Glucose	30.0–1.80	65,187	98.0	3.2	16.1	6.0
	1.88–1.80 ^b	7621	93.5	1.9	4.7	16.5
Fucose	30.0–1.80	66,843	97.5	2.6	15.3	4.7
	1.88–1.80	7954	94.4	2.1	3.1	24.6
Quinovose	30.0–1.85	60,834	96.4	2.2	12.0	6.3
	1.93–1.85	6968	94.1	1.7	3.0	25.1
L-Arabinose	30.0–1.80	65,141	95.3	2.4	13.0	5.2
	1.88–1.80	7431	88.2	1.9	2.5	27.3
Xylose	30.0–1.90	55,244	94.0	2.6	10.2	7.2
	1.99–1.90	6116	84.3	1.8	2.8	24.3

^a $R_{\text{sym}} = (\Sigma |I - \bar{I}| / \Sigma I) \times 100$.

^b Statistics for the highest resolution bin.

50 kV and 90 mA. The x-ray data were processed with SAINT (Bruker AXS, Inc.) and internally scaled with XSCALIBRE.² X-ray data collection statistics are presented in Table I.

The structures of the enzyme-sugar complexes were analyzed by difference Fourier techniques. Iterative cycles of refinement with the software package TNT (23) and manual model building with the program TURBO (24) reduced the R -factors to 17.2% or lower for all x-ray data sets. Refinement statistics are presented in Table II.

Kinetic Measurements and Analysis—The enzymatic activity of wild-type mutarotase was measured with a DIP-360 digital polarimeter (Jasco) at 25 °C. The change in a specific rotation of each substrate was measured as the α -anomer was converted to the equilibrium mixture of isomers, except for L-arabinose where the starting substrate was the β -anomer. All substrates were rapidly dissolved in 25 mM Hepes (pH 7.6) and 50 mM KCl immediately before addition of the enzyme. The rate of the non-enzymatic turnover was subtracted from the initial rate of the enzymatic reaction. The kinetic constants were determined by fitting the experimental velocity data to Equation 1, where V_{max} is the maximal velocity, K_m is the Michaelis constant, and A is the substrate concentration. The data are presented in Table III.

$$v/E_t = V_{\text{max}}A/(K_m + A) \quad (\text{Eq. 1})$$

RESULTS AND DISCUSSION

The crystals of *L. lactis* galactose mutarotase employed in this investigation contained one dimer per asymmetric unit. For the sake of simplicity the following discussion will refer only to Subunit II in the x-ray coordinate files unless otherwise indicated. Shown in Fig. 2 is the electron density corresponding to the glucose ligand observed in the mutarotase-glucose com-

plex. Unlike that observed for galactose, the electron density corresponding to the C-1 hydroxyl group of glucose indicates that only the β -anomeric configuration of the ligand is present in the active site. Indeed, the α -anomeric configuration cannot be accommodated in this binding mode due to a steric clash with the aromatic side chain of Phe-279.

A superposition of the mutarotase active sites with either bound glucose or galactose is displayed in Fig. 3. The α -carbons for the two protein-sugar complexes correspond with a root mean square deviation of 0.32 Å. As can be seen there are virtually no structural differences between the proteins with either glucose or galactose situated in their respective active sites. Strikingly and unexpectedly, however, the sugar ligands bind in completely different manners. Specifically, as shown in Fig. 3, C-4 of galactose nearly superimposes onto the C-5 ring oxygen of glucose. The C-1 hydroxyl group of glucose is no longer situated within hydrogen bonding distance of His-96, His-170, and Glu-304. Rather, it lies within 2.9 Å of Arg-71, 2.9 Å of Glu-203, 2.6 Å of Asp-243, and 2.9 Å of a solvent molecule. Due to this change in orientation, the C-6 hydroxyl group of glucose is now positioned within 2.8 Å of His-96, 2.8 Å of His-170, and 2.8 Å of a solvent molecule.

Schematics of the hydrogen bonding patterns exhibited between the mutarotase and either galactose or glucose are shown in Fig. 4, *a* and *b*, respectively. In the case of galactose, five amino acid residues play critical roles in ligand binding: Arg-71 and Asp-243 on the left side of the pocket and His-96, His-170, and Glu-304 on the right side. Additionally four or-

² I. Rayment and G. Wesenberg, unpublished data.

TABLE II
Relevant least squares refinement statistics

Complex	D-Glucose	D-Fucose	D-Quinovose	L-Arabinose	D-Xylose
Resolution limits (Å)	30.0–1.80	30.0–1.80	30.0–1.85	30.0–1.80	30.0–1.90
R-factor (overall) (%) ^a	15.9	17.1	17.1	17.2	16.8
(no. rflns)	(65,035)	(66,687)	(60,782)	(65,180)	(55,169)
R-factor (work) (%)	15.5	16.8	16.8	16.9	16.5
(no. rflns)	(58,576)	(59,987)	(54,673)	(58,551)	(49,622)
R-factor (free) (%)	23.1	22.9	22.7	23.0	22.3
(no. rflns)	(6459)	(6700)	(6109)	(6629)	(5547)
No. protein atoms	5397 ^b	5406 ^c	5394 ^d	5390 ^e	5389 ^f
No. hetero-atoms	1036 ^g	531 ^h	479 ⁱ	456 ^j	452 ^k
Weighted root mean square deviations from ideality					
Bond lengths (Å)	0.013	0.012	0.013	0.013	0.011
Bond angles (degree)	2.21	2.26	2.31	2.17	2.26
Trigonal planes (Å)	0.007	0.007	0.007	0.006	0.006
General planes (Å)	0.013	0.012	0.012	0.014	0.011
Torsional angles (degree) ^l	18.0	18.6	18.7	18.7	18.8

^a R-factor = $(\sum |F_o - F_c| / \sum |F_o|) \times 100$, where F_o is the observed structure-factor amplitude, and F_c is the calculated structure-factor amplitude.

^b These include multiple conformations for Lys-52, Ser-140, Lys-199, Val-205, Glu-292, and Ser-335 in Subunit I and Lys-42 and Thr-338 in Subunit II.

^c These include multiple conformations for Lys-4, Ser-26, Lys-73, Ser-140, and Glu-292 in Subunit I and Lys-78, Met-139, Asp-285, Glu-316, and Glu-326 in Subunit II.

^d These include multiple conformations for Lys-4, Ser-26, and Ser-140 in Subunit I and Lys-78, Ser-101, Asp-285, Glu-316, and Glu-326 in Subunit II.

^e These include multiple conformations for Lys-4, Ser-140, and Asp-264 in Subunit I and Lys-4, Glu-316, and Glu-326 in Subunit II.

^f These include multiple conformations for Gln-237 in Subunit I and Asp-285, Glu-316, Glu-326, and His-347 in Subunit II.

^g These include 1011 water molecules, two glucose molecules, and one sodium ion.

^h These include 506 water molecules, two fucose molecules, and one sodium ion.

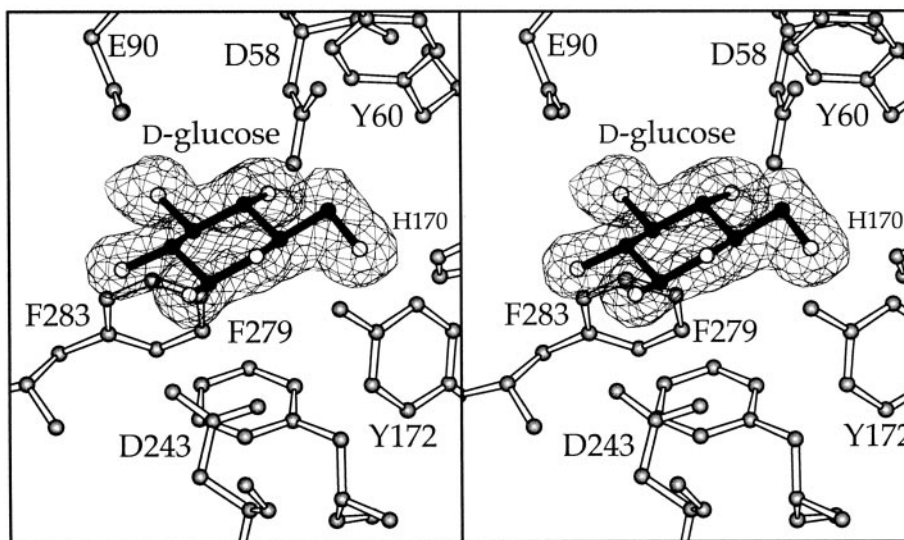
ⁱ These include 456 water molecules, two quinovose molecules, and one sodium ion.

^j These include 434 water molecules, two L-arabinose molecules, and one sodium ion.

^k These include 430 water molecules, two xylose molecules, and one nickel(II) ion.

^l These were not restrained during the course of the refinements.

FIG. 2. **Electron density corresponding to D-glucose bound in Subunit II of the dimer.** The map shown was calculated with coefficients of the form $(F_o - F_c)$, where F_o was the native structure factor amplitude and F_c was the calculated structure factor amplitude from the model lacking the coordinates for the sugar ligand. The map was contoured at 2.5σ . The average B-values for the glucose molecules in Subunits I and II were 19.4 and 20.3 Å², respectively.

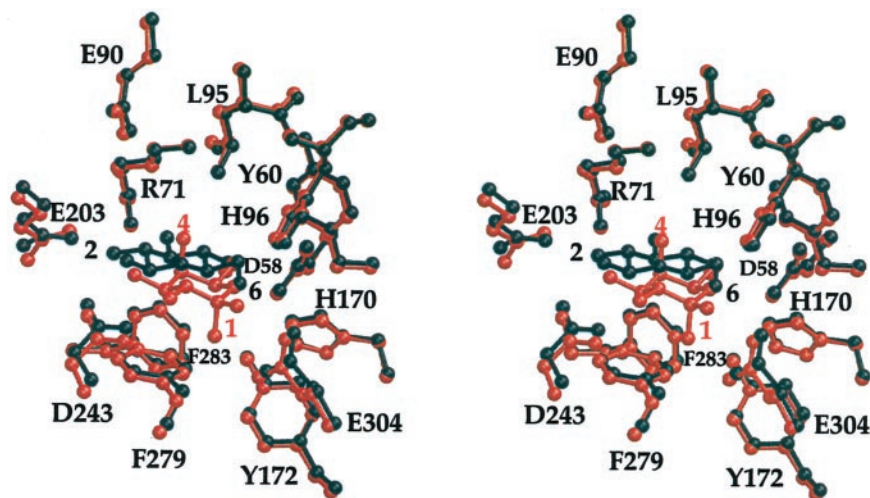


dered water molecules lie within hydrogen bonding distance to galactose, one of which serves to bridge the C-2 and C-1 hydroxyl (β -anomer) groups. Approximately 28% of the surface area of galactose is buried by the protein as calculated according to the algorithm of Lee and Richards (25). When glucose binds within the mutarotase active site, five amino acid residues are again critical for binding, four of which are the same as for galactose (Arg-71, Asp-243, His-96, and His-170). With respect to glucose binding, eight ordered water molecules are located within hydrogen bonding distance of the sugar. The alternate binding mode exhibited by glucose results in the sugar being directed out toward the solvent with an approximate 5% reduction in its buried surface area. Importantly, when galactose binds in the mutarotase active site, the C-4 hydroxyl moiety is positioned within hydrogen bonding distance of Arg-71. In contrast, when glucose is bound to the

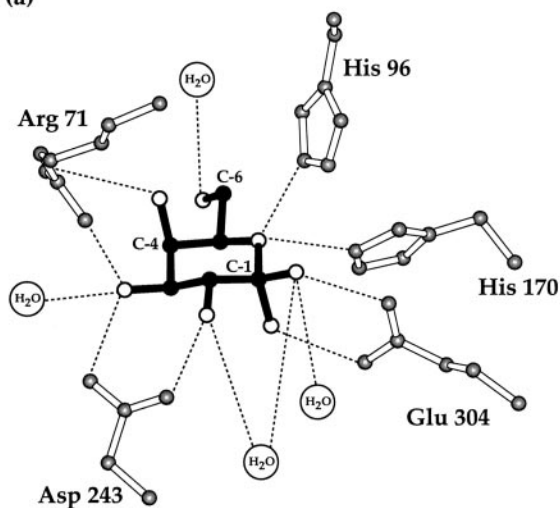
enzyme, the C-4 hydroxyl group is surrounded only by two water molecules located within 2.5 and 2.8 Å.

The unexpected manner in which glucose bound in the active site of galactose mutarotase emphasizes the need for caution in interpreting x-ray data in the absence of accompanying biochemical and kinetic data. Clearly the use of substrate analogs has had a profound impact on our present day understanding of enzyme structure and function. Nevertheless, the results must be approached with caution, since the compounds employed in such studies are not true substrates or intermediates and may not fit into the active site in a manner that mimics true substrate binding. In the present work this is illustrated by glucose, a known but perhaps not physiologically relevant substrate. Indeed, based on the mode of glucose binding to the enzyme and in the absence of the previous x-ray crystallographic investigation on the mutarotase-galactose complex, it

FIG. 3. Superpositions of the mutarotase active sites with either bound glucose or galactose. The structure of the mutarotase/galactose complex is shown in red while that of the enzyme/glucose complex is depicted in black.



(a)



(b)

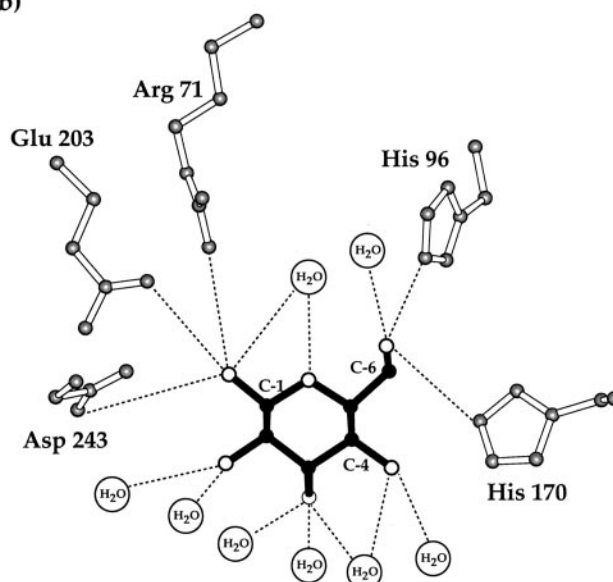


FIG. 4. Schematic diagrams of the hydrogen bonding patterns between the protein and either galactose or glucose. Possible hydrogen bonds (3.2 Å or less) between the protein and either galactose or glucose are indicated by the dashed lines in a and b, respectively.

TABLE III

Kinetic constants for galactose mutarotase from *L. lactis*

Assay solutions contained 25 mM Hepes (pH 7.6), 50 mM KCl, and varying amounts of substrate. Assays were performed at 25 °C.

Sugars	k_{cat} s^{-1}	K_m mM	k_{cat}/K_m $\text{m}^{-1} \text{s}^{-1}$
D-Galactose	3700 ± 240	20 ± 3	1.85×10^5
D-Glucose	430 ± 32	34 ± 6	0.13×10^5
D-Fucose	1700 ± 120	25 ± 4	0.68×10^5
D-Quinovose	490 ± 30	37 ± 7	0.13×10^5
L-Arabinose	5500 ± 600	32 ± 9	1.72×10^5
D-Xylose	410 ± 38	21 ± 5	0.20×10^5

might have been speculated that Asp-243, Glu-203, and Arg-71 rather than His-96, His-170, and Glu-304 play key catalytic roles. Based on preliminary unpublished kinetic data for various site-directed mutant proteins examined in our laboratories, however, it appears that Glu-304 and His-170 are critically important for catalysis with all sugar substrates, whereas Asp-243 is not important and His-96 is somewhere in between.

As indicated in Table III, the k_{cat} and K_m values with α -D-galactose as a substrate were $3700 \pm 240 \text{ s}^{-1}$ and $20 \pm 3 \text{ mM}$,

respectively. For α -D-glucose as the substrate, the k_{cat} and K_m values were $430 \pm 32 \text{ s}^{-1}$ and $34 \pm 6 \text{ mM}$, respectively. Most likely the reduction in k_{cat} with glucose as the substrate is a function of its non-productive binding as demonstrated in this x-ray crystallographic analysis. The question arises as to why this alternate binding mode occurs for glucose and not for galactose. In the complex of the enzyme with bound galactose, the C-4 hydroxyl sugar is in the proper orientation to form a hydrogen bond with the guanidinium group of Arg-71 (3.2 Å). When glucose binds to the enzyme in the same manner as galactose, and presumably this occurs, since galactose mutarotase is active against glucose, the interaction with Arg-71 is absent due to the different spatial orientation of the C-4 hydroxyl group (Scheme 2). It can thus be speculated that the guanidinium group of Arg-71, through its interactions with the C-4 hydroxyl group of galactose, plays a key role in the reaction mechanism by directing the sugar into the proper orientation for efficient catalysis. Without this interaction, alternate binding modes occur as shown here for the mutarotase-glucose complex. The different binding modes for glucose versus galactose clearly emphasize the importance of even a single hydrogen bond in protein-carbohydrate interactions.

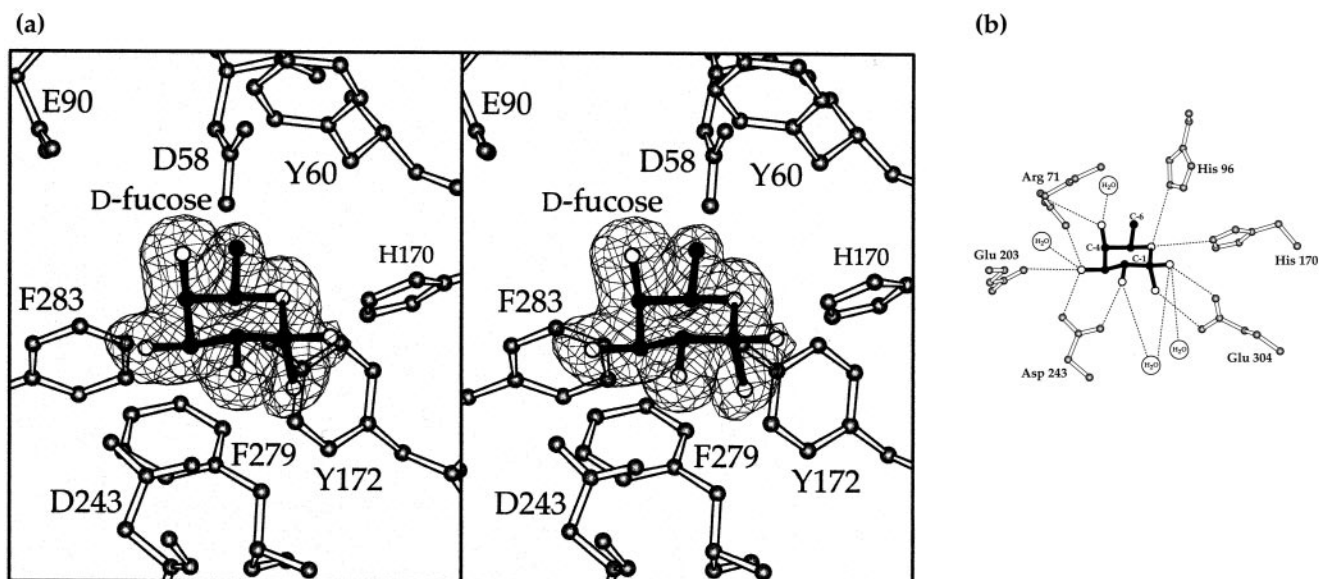


FIG. 5. The *L. lactis* active site with bound D-fucose. Shown in *a* is the electron density corresponding to D-fucose when bound to Subunit II of the dimer. The map shown was calculated as described in the legend to Fig. 2. The average temperature factors for the fucose moieties were 18.9 and 19.4 Å² in Subunits I and II, respectively. A schematic representation of the hydrogen bonding pattern exhibited between the sugar and the enzyme is given in *b*. Dashed lines indicate possible electrostatic interactions within 3.2 Å.

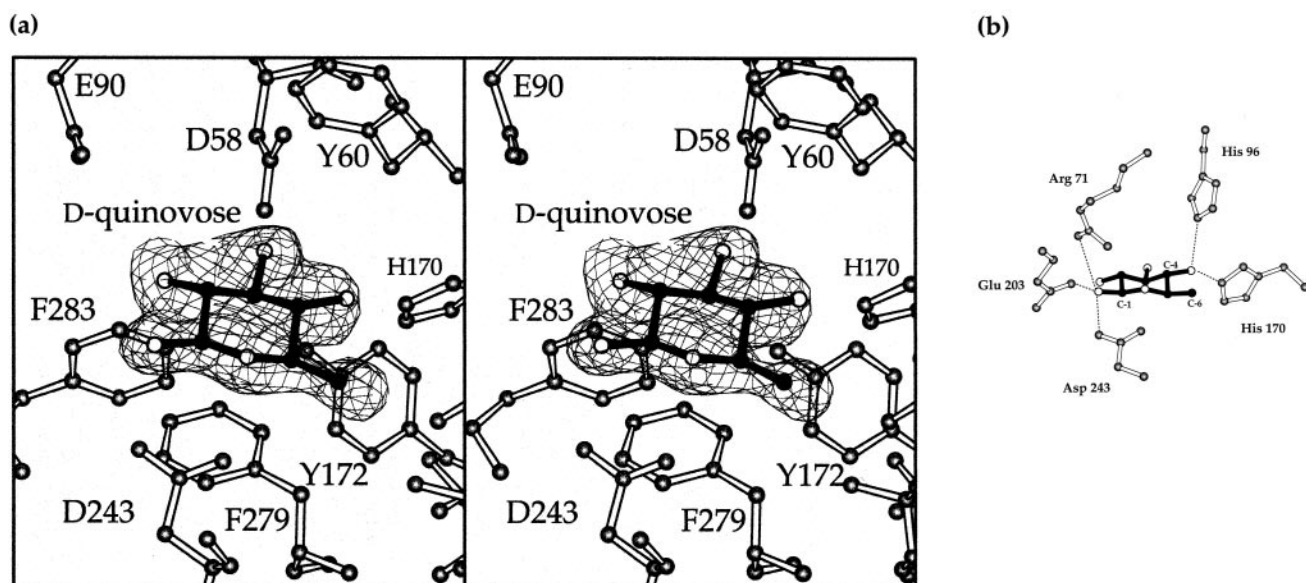


FIG. 6. The *L. lactis* active site with bound D-quinovose. Shown in *a* is the electron density corresponding to D-quinovose when bound to Subunit II of the dimer. The temperature factors for the quinovose ligands in Subunits I and II were 37.4 and 39.7 Å², respectively. A schematic representation of the hydrogen bonding pattern formed between the sugar and the enzyme is given in *b*. Dashed lines indicate possible electrostatic interactions within 3.2 Å.

If, as suggested, Arg-71 plays a critical role for properly positioning the sugar ligand in the active site for efficient catalysis, then it can be predicted that those sugars, which mimic the hydroxyl configuration of glucose about C-4, will bind like glucose in the crystalline enzyme. Correspondingly, those sugars that mimic galactose will maintain the hydrogen bond with Arg-71 and thus bind like galactose. Furthermore, it might be expected that the catalytic rates for those sugars mimicking galactose will be higher than those mimicking glucose. To test this hypothesis, the next set of sugars studied in this investigation were α -D-fucose and α -D-quinovose, which represent C-6 deoxy sugar analogs of galactose and glucose, respectively (Scheme 2).

Shown in Fig. 5*a* is the electron density corresponding to D-fucose when bound to galactose mutarotase. The α -carbons

for the proteins with bound galactose versus fucose superimpose with a root mean square deviation of 0.13 Å. As can be seen, the electron density map shows that both the α - and β -anomers of the sugar are present in the active site. Also, as predicted, the sugar binds in the active site pocket in the same orientation as galactose with its C-1 hydroxyl group located within hydrogen bonding distance of Glu-304 and the guanidinium group of Arg-71 situated within hydrogen bonding distance to its C-4 hydroxyl group (Fig. 5*b*). Indeed, the overall hydrogen bonding pattern observed between the protein and fucose as shown in Fig. 5*b* is virtually identical to that between the protein and galactose as outlined in Fig. 4*a*. Clearly the loss of the C-6 hydroxyl group in fucose has little effect on the binding of the ligand to the crystalline enzyme as would be expected, since, in galactose, the C-6 hydroxyl group does not

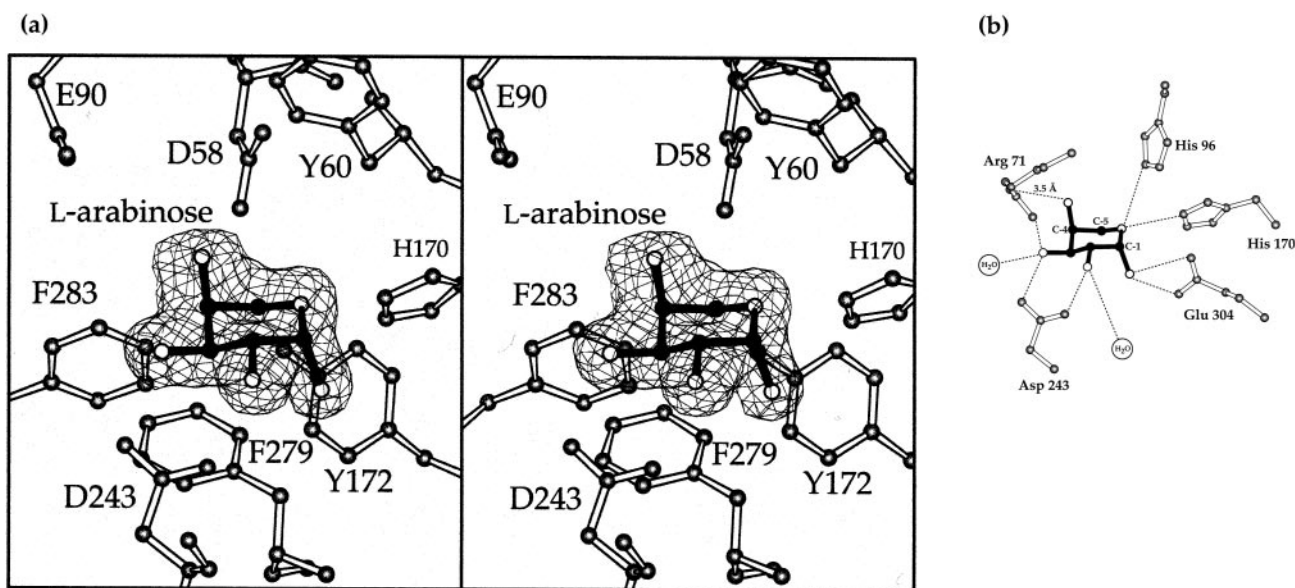


FIG. 7. The *L. lactis* active site with bound L-arabinose. Shown in *a* is the electron density corresponding to L-arabinose when bound to Subunit II of the dimer. The temperature factors for the L-arabinose ligands in Subunits I and II were 28.7 and 30.3 Å², respectively. A schematic representation of the hydrogen bonding pattern observed between the sugar and the enzyme is given in *b*. Dashed lines indicate possible electrostatic interactions within 3.2 Å.

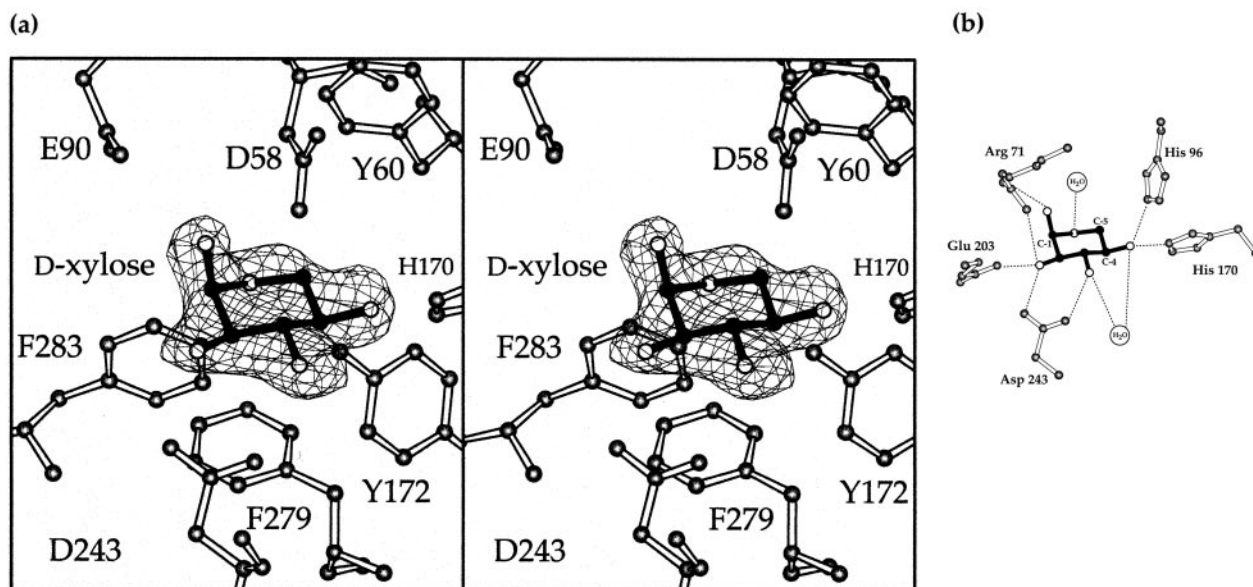


FIG. 8. The *L. lactis* active site with bound D-xylose. Shown in *a* is the electron density corresponding to D-xylose when bound to Subunit II of the dimer. The temperature factors for the xylose moieties were 36.7 and 36.3 Å², respectively, for Subunits I and II and are similar to those observed for quinovose. A schematic representation of the hydrogen bonding pattern formed between the sugar and the enzyme is given in *b*. Dashed lines indicate possible electrostatic interactions within 3.2 Å.

make specific interactions with the protein but rather is surrounded by water molecules. The k_{cat} and K_m values with α -D-fucose as the substrate were $1700 \pm 120 \text{ s}^{-1}$ and $25 \pm 4 \text{ mM}$, respectively.

The electron density corresponding to quinovose when bound to the enzyme is depicted in Fig. 6*a*. Only the β -anomer of the sugar is observed in the active site, presumably due to the steric hindrance imposed by the aromatic side chain of Phe-279. The α -carbons for the enzyme-quinovose *versus* enzyme-galactose complexes superimpose with a root mean square deviation of 0.13 Å. In sharp contrast to the other sugars, there are only five potential electrostatic interactions between the protein and quinovose, as depicted in Fig. 6*b*. Like that observed with bound glucose in the active site, the C-1 hydroxyl group of quinovose lies within 3.1 Å of Arg-71, 2.9 Å of Glu-203,

and 2.8 Å of Asp-243 (Figs. 4*b* and 6*b*). In sharp contrast, however, the C-4 hydroxyl of quinovose is anchored to the protein via the imidazole nitrogens of His-96 and His-170. In glucose, these same protein side chains serve to anchor the C-6 hydroxyl group, which is missing in quinovose. As a result, the binding mode for quinovose lies somewhere between that observed for glucose and for galactose. The k_{cat} for quinovose is considerably reduced at $490 \pm 30 \text{ s}^{-1}$.

As the next step in this investigation, the molecular structures of galactose mutarotase complexed with either L-arabinose or D-xylose were determined. These sugars represent the five-carbon analogs of galactose and glucose, respectively. The electron density corresponding to L-arabinose bound in the active site of Subunit II is displayed in Fig. 7*a*. Note that, as opposed to Subunit II, the sugar adopts both anomeric forms

in Subunit I (not shown). Possible electrostatic interactions between the sugar and the protein are highlighted in Fig. 7*b*. Not surprisingly, these interactions are similar to those observed for galactose (Fig. 4*a*). The distance between the C-4 hydroxyl group of L-arabinose and N^η2 of Arg is ~3.5 Å and, within experimental error, is similar to that observed for galactose (3.2 Å). The α-carbons for the enzyme complexed with galactose *versus* L-arabinose correspond with a root mean square deviation of 0.13 Å. As judged by the kinetic constants presented in Table III, L-arabinose is as good a substrate for galactose mutarotase as galactose, thus highlighting the importance of the hydroxyl configuration about C-4 for proper sugar positioning in the active site region.

The mode of binding of D-xylose to galactose mutarotase is shown in Fig. 8, *a* and *b*. The kinetic constants with D-xylose as the substrate are similar to those of glucose and quinovose. The C-4 hydroxyl group of xylose lies within hydrogen bonding distance of His-96 and His-170, which is similar to that observed with quinovose (Fig. 6*b*). However, the xylose moiety is “flipped” with respect to quinovose in the active site such that its C-1 hydroxyl group now lies within hydrogen bonding distance of Arg-71, and its C-2 and C-3 hydroxyl groups are anchored to the protein via the carboxylate group of Asp-243. This alternate mode of binding is reflected in the kinetic constants listed in Table III.

From the five enzyme-sugar complexes described here, it is apparent that the orientation of the C-4 hydroxyl group dictates the manner in which the ligand is trapped in the crystalline enzyme. Accordingly, when the C-4 hydroxyl group of the sugar is in the “galactose” orientation, the C-1 hydroxyl group orients toward His-96, His-170, and Glu-304, and these sugars of the “galactose family” are the best substrates for the enzyme. Apparently, the hydrogen bond between Arg-71 and the C-4 hydroxyl groups of D-galactose, D-fucose, or L-arabinose serves to steer the sugar into the orientation required for catalysis. In sharp contrast, when the C-4 hydroxyl groups of the sugars are in the “glucose” configuration, the molecules bind in alternate

orientations, at least in the crystalline enzyme, and these “non-productive” modes are reflected in the measured kinetic parameters as listed in Table III.

Acknowledgment—We thank Dr. John Lindquist (Department of Bacteriology, University of Wisconsin-Madison) for supplying *L. lactis* var. *lactis* cell stock.

REFERENCES

1. Bouffard, G. G., Rudd, K. E., and Adhya, S. L. (1994) *J. Mol. Biol.* **244**, 269–278
2. Bentley, R., and Bhate, D. S. (1960) *J. Biol. Chem.* **235**, 1219–1224
3. Bentley, R., and Bhate, D. S. (1960) *J. Biol. Chem.* **235**, 1225–1233
4. Wallenfels, K., and Herrman, K. (1965) *Biochem. Z.* **343**, 294–306
5. Keston, A. S. (1963) *Arch. Biochem. Biophys.* **102**, 306–312
6. Li, L. K. (1965) *Arch. Biochem. Biophys.* **110**, 156–162
7. Lapedes, S. L., and Chase, A. M. (1968) *Biochem. Biophys. Res. Commun.* **31**, 967–972
8. Bailey, J. M., Fishman, P. H., and Pentchev, P. G. (1967) *J. Biol. Chem.* **242**, 4263–4269
9. Bailey, J. M., Fishman, P. H., and Pentchev, P. G. (1969) *J. Biol. Chem.* **244**, 781–788
10. Gatz, C., Altschmied, J., and Hillen, W. (1986) *J. Bacteriol.* **168**, 31–39
11. Poolman, B., Royer, T. J., Mainzer, S. E., and Schmidt, B. F. (1990) *J. Bacteriol.* **172**, 4037–4047
12. Mollet, B., and Pilloud, N. (1991) *J. Bacteriol.* **173**, 4464–4473
13. Maskell, D. J., Szabo, M. J., Deadman, M. E., and Moxon, E. R. (1992) *Mol. Microbiol.* **6**, 3051–3063
14. Erlandson, K. A., Delamarre, S. C., and Batt, C. A. (2001) *Appl. Environ. Microbiol.* **67**, 1445–1452
15. Hucho, F., and Wallenfels, K. (1971) *Eur. J. Biochem.* **23**, 489–496
16. Thoden, J. B., and Holden, H. M. (2002) *J. Biol. Chem.* **277**, 20854–20861
17. Jacobson, R. H., Zhang, X. J., DuBose, R. F., and Matthews, B. W. (1994) *Nature* **369**, 761–766
18. Parsons, M. R., Convery, M. A., Wilmot, C. M., Yadav, K. D., Blakeley, V., Corner, A. S., Phillips, S. E., McPherson, M. J., and Knowles, P. F. (1995) *Structure* **3**, 1171–1184
19. Li, S., Kelly, S. J., Lamani, E., Ferraroni, M., and Jedrzejewski, M. J. (2000) *EMBO J.* **19**, 1228–1240
20. Féthière, J., Eggimann, B., and Cygler, M. (1999) *J. Mol. Biol.* **288**, 635–647
21. Egloff, M.-P., Uppenberg, J., Haalck, L., and van Tilbeurgh, H. (2001) *Structure (Lond.)* **9**, 689–697
22. Keston, A. S. (1954) *Science* **120**, 355–356
23. Tronrud, D. E., Ten Eyck, L. F., and Matthews, B. W. (1987) *Acta Crystallogr. Sect. A* **43**, 489–501
24. Roussel, A., Fontecilla-Camps, J. C., and Cambillau, C. (1990) *Acta Crystallogr. Sect. A* **46**, C66–C67
25. Lee, B., and Richards, F. M. (1971) *J. Mol. Biol.* **55**, 379–400
26. Kraulis, P. J. (1991) *J. Appl. Crystallogr.* **24**, 946–950